Parton Distribution Functions from Ioffe time pseudo-distributions from lattice caclulations; approaching the physical point

Bálint Joó,[1] Joseph Karpie,[2] Kostas Orginos,[1,3]
Anatoly V. Radyushkin,[1,4] David G. Richards,[1] and Savvas Zafeiropoulos[5]

[1] *Thomas Jefferson National Accelerator Facility, Newport News, VA 23606, USA*
[2] *Physics Department, Columbia University, New York City, New York 10027, USA*
[3] *Physics Department, College of William and Mary, Williamsburg, Virginia 23187, USA*
[4] *Physics Department, Old Dominion University, Norfolk, VA 23529, USA*
[5] *Aix Marseille Univ, Université de Toulon, CNRS, CPT, Marseille, France*

We present results for the unpolarized parton distribution function of the nucleon computed in lattice QCD at the physical pion mass. This is the first study of its kind employing the method of Ioffe time pseudo-distributions. Beyond the reconstruction of the Bjorken-x dependence we also extract the lowest moments of the distribution function using the small Ioffe time expansion of the Ioffe time pseudo-distribution. We compare our findings with the pertinent phenomenological determinations.

PACS numbers: 12.38.-t, 11.15.Ha, 12.38.Gc

Introduction.— The determination and understanding of the internal quark and gluon structure of the proton is a crucial aspect of the precision phenomenology program of the current and future hadron collider experiments, especially the upcoming Electron-Ion Collider (EIC). The framework of collinear factorization quantifies the hadronic structure in terms of Parton Distribution Functions (PDFs) which encapsulate the pertinent information regarding the momentum distributions of quarks and gluons within the nucleon. Till very recently, the intrinsic non-perturbative nature of the PDFs was prohibiting an ab-initio computation and the conventional approach is to employ a variety of experimental data together with advanced fitting methodologies in order to extract the PDFs via global fits. The studies of PDFs are of paramount importance precisely due to the fact that their uncertainties play a crucial role in many LHC applications. They affect the measurement of precision SM parameters, such as the W mass, the strong coupling constant and the determination of the couplings of the Higgs boson where discrepancies from the stringently fixed SM predictions would serve as indisputable evidence of BSM physics [1].

The possibility to determine the PDFs with first principle lattice calculations is the object of a long endeavor which recently lead to a culmination of results. The crux of the difficulties impeding a first principle implementation was actually associated with the fact that the matrix elements defining the PDFs involve light-cone separated fields. In his seminal article that stimulated the recent efforts, X. Ji [2] proposed to compute matrix elements of fields separated by a purely space-like distance $z = z_3$ that define the so-called quasi-PDF, the distributions in the longitudinal momentum p_3. In the large p_3 limit, they can be factorized into the light-cone PDF, $f(x, \mu^2)$. Subsequently, many articles studying quasi-PDFs, as well as the pion quasi-distribution amplitude (DA) appeared in the literature [3–20].

Alternative approaches based on the analysis of equal-time current correlators [21–24] also aim to study the PDFs or DAs in lattice QCD. "Good Lattice Cross-Sections" (LCS), as described in [25], represent a general framework, where one computes matrix elements that can be factorized into PDFs at short distances. Works of [26–30] fall into these categories. For comprehensive reviews on the topic, we refer the reader to [31–34].

Ioffe time pseudo-distributions.—

Another position-space formulation was proposed in [35]. In this approach, the basic object is the Ioffe time pseudo-distribution function (pseudo-ITD) $\mathcal{M}(\nu, z^2)$. The Lorentz invariant $\nu = p \cdot z$ is known as the Ioffe time [36, 37]. The pseudo-ITD is the invariant amplitude for a matrix element with space-like separated quark fields.

In renormalizable theories, the pseudo-ITD exhibits a logarithmic singularity at small values of z^2. These short-distance singularities can be factorized into the PDF and a perturbatively calculable coefficient function. The pseudo-ITD can also be considered as a LCS. A series of works implemented this formalism and studied its efficiency [38–43]. For the sake of completeness, the main points of our formalism are summarized below, but we refer the reader to [42, 44] for a detailed discussion.

The non-local matrix element,

$$M^\alpha(p, z) = \langle p|\bar{\psi}(z)\gamma^\alpha U(z; 0)\psi(0)|p\rangle\,, \tag{1}$$

with U being a straight Wilson line, $p = (p^+, \frac{m^2}{2p^+}, 0_T)$, $z = (0, z_-, 0_T)$ and $\gamma^a = \gamma^+$ in light-cone coordinates, defines the $\overline{\text{MS}}$ ITD (introduced in [37]), given a regularization is made for the $z^2 = 0$ singularity. For $z^2 \neq 0$, this matrix element has the following Lorentz decomposition

$$M^\alpha(z, p) = 2p^\alpha \mathcal{M}(\nu, z^2) + 2z^\alpha \mathcal{N}(\nu, z^2)\,. \tag{2}$$

The pseudo-ITD $\mathcal{M}(\nu, z^2)$ contains the leading twist contribution, while $\mathcal{N}$ is an entirely higher-twist term. In the kinematics $p = (E, 0, 0, p_3)$, $z = (0, 0, 0, z_3)$, the smart choice $\alpha = 0$ isolates $\mathcal{M}$. Nonetheless, it still contains higher twist contaminations $O(z^2\Lambda^2_{\rm QCD})$. In the limit of small z^2, where higher twist terms are suppressed, $\mathcal{M}$ is factorizable into the ITD (or equivalently, the PDF) and a perturbative coefficient function, provided that one removes Wilson line-related UV divergences that appear at finite z^2. These UV divergences are eliminated if one considers the reduced pseudo-ITD [35, 38] given by the ratio

$$\mathfrak{M}(\nu, z^2) = \frac{\mathcal{M}(\nu, z^2)}{\mathcal{M}(0, z^2)}\,. \tag{3}$$

It contains the same singularities in the $z^2 = 0$ limit as $\mathcal{M}$, and can be related to the $\overline{\rm MS}$ light-cone ITD by the NLO matching relation [45–47]

$$\begin{aligned}\mathfrak{M}(\nu, z^2) =& Q(\nu, \mu^2) - \frac{\alpha_s C_F}{2\pi}\int_0^1 du\, Q(u\nu, \mu^2)\times \\ & \left[\ln\left(z^2\mu^2\frac{e^{2\gamma_E+1}}{4}\right)B(u) + L(u)\right],\end{aligned} \tag{4}$$

where $B(u) = \left[\frac{1+u^2}{1-u}\right]_+$ is the Altarelli-Parisi kernel [48], and

$$L(u) = \left[4\frac{\ln(1-u)}{1-u} - 2(1-u)\right]_+ \tag{5}$$

is the non-logarithmic part.

Extracting the matrix element — The numerical computation of our matrix elements relies on Gaussian smearing [51] and momentum-smearing [52] for constructing the nucleon interpolating field, as well as the summation method for better control of the excited state contamination. The latter is intimately related to the Feynman-Hellmann (FH) theorem [53] and has been widely used in Lattice calculations of PDFs [17, 18, 38, 39, 42, 43, 54].

The matrix element is determined from a ratio of correlation functions

$$R(t) = \frac{\sum_\tau C_3(t, \tau)}{C_2(t)}\,. \tag{6}$$

where $C_{2,3}$ are standard two and three point correlation functions, t is the Euclidean separation between the source and sink interpolating fields and the operator insertion time τ is summed over the entire temporal range. The effective matrix element $M^{\rm eff}$ is then constructed as

$$M^{\rm eff}(t) = R(t+1) - R(t)\,. \tag{7}$$

The leading excited-state effects can be parameterized by

$$M^{\rm eff}(t) = M(1 + \sum_i A_i e^{-\Delta t} + B_i t e^{-\Delta t})\,. \tag{8}$$

with Δ being the energy gap between the ground state and the lowest excited state.

The summation method has a clear advantage over the typical ratio method. The excited state contamination scales as $\exp(-\Delta t)$ instead of $\exp(-\Delta t/2)$, which allows for smaller t to be used to control excited state effects. This is a major advantage considering that the correlation functions' signal-to-noise ratio decays exponentially in t. This means that if N measurements are required to reach a specific statistical precision for the correlator at $t_{\rm rat}$ with the ratio method, only $\sqrt{N}$ measurements are required to reach the same precision at time $t_{\rm sum} = t_{\rm rat}/2$ for the summation method. In both cases the contamination from excited states is the same. This feature is important for calculations at high hadron momentum where excited state energy gaps can be small and the signal-to-noise ratio decays much faster than for low momentum states.

Lattice QCD calculation. — In this study three ensembles of configurations with lattice spacing $a = 0.094$ fm with decreasing value of the pion mass have been employed. In Tab. I, we list all the parameters of our analysis. The pion masses of this study are 172 MeV, 278 MeV, and 390 MeV. These ensembles allow for a controlled extrapolation to the precise physical pion mass which constitutes an important limit to be taken in order to safely compare with the PDF determinations of global fits but also for the first time we can study the pion mass effects on the ITD. As was done in [42], correlation functions with several different smearings were simultaneously fit to determine the matrix element from Eq. (8). The matrix elements extracted from fitting correlation functions to Eq. (8) are shown in Fig. 1.

Moments of the PDF — Following our suggestion in [40], we can use the reduced pseudo-ITD to compute the moments of the PDF. Valuable information for the PDF can be extracted from the data without dealing with the pitfalls of the inverse problem. The moments of the $\overline{\rm MS}$ PDF, $a_n(\mu^2)$, are related multiplicatively to those of the Fourier transform of the reduced pseudo-ITD,

$$b_n(z^2) = C_n(\mu^2 z^2)a_n(\mu^2) + \mathcal{O}(z^2\Lambda^2_{\rm QCD}) \tag{9}$$

where C_n are the Mellin moments of the matching kernel $C(u, \mu^2 z^2)$ with respect to u. To NLO accuracy,

$$C_n(z^2\mu^2) = 1 - \frac{\alpha_s}{2\pi}C_F\left[\gamma_n \ln\left(z^2\mu^2\frac{e^{2\gamma_E+1}}{4}\right) + l_n\right], \tag{10}$$

where

$$\gamma_n = \int_0^1 du\, B(u)u^n = \frac{1}{(n+1)(n+2)} - \frac{1}{2} - 2\sum_{k=2}^{n+1}\frac{1}{k}\,, \tag{11}$$

ID	a(fm)	M_π(MeV)	β	$c_{\rm SW}$	am_l	am_s	$L^3 \times T$	$N_{\rm cfg}$
$a091m390$	0.094(1)	390(71)	6.3	1.20536588	-0.2350	-0.2050	$32^3 \times 64$	417
$a091m280$	0.094(1)	278(3)	6.3	1.20536588	-0.2390	-0.2050	$32^3 \times 64$	500
$a091m170$	0.094(1)	172(6)	6.3	1.20536588	-0.2416	-0.2050	$64^3 \times 128$	175

TABLE I. Parameters for the lattices generated by the JLab/W&M collaboration [49] using 2+1 flavors of stout-smeared clover Wilson fermions and a tree-level tadpole-improved Symanzik gauge action. More details about these ensembles can be found in [50].

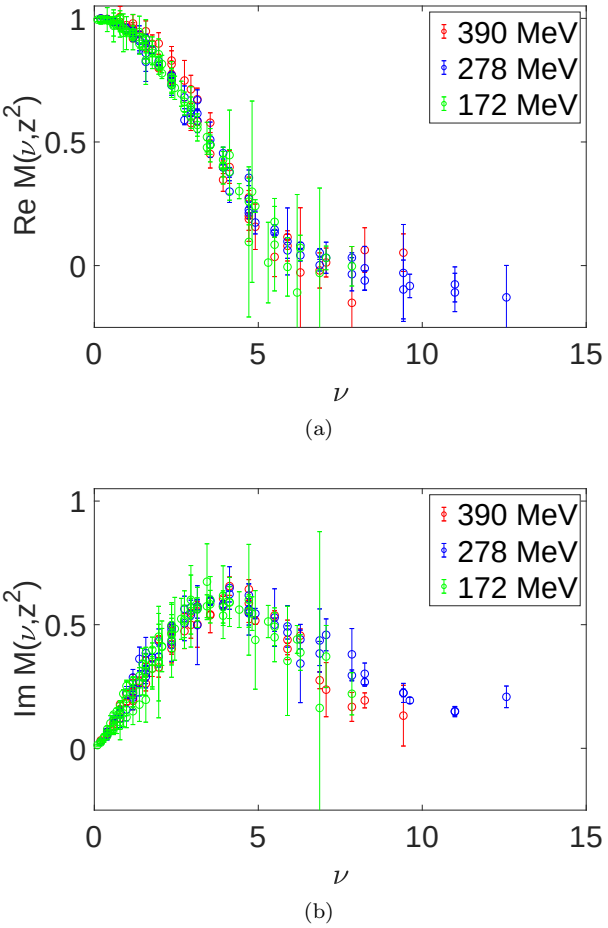

FIG. 1. The reduced pseudo-ITD calculated on ensembles with 390 MeV, 278 MeV, and 172 MeV pion masses. The upper and lower plots are the real and imaginary component respectively. There appears to be very small mass effects within this range of ν and z^2.

are the moments of the Altarelli-Parisi kernel, and

$$l_n = \int_0^1 du\, L(u) u^n = 2\left[\left(\sum_{k=1}^{n}\frac{1}{k}\right)^2 + \sum_{k=1}^{n}\frac{1}{k^2} + \frac{1}{2} - \frac{1}{(n+1)(n+2)}\right]. \quad (12)$$

The even and odd moments can be determined from the coefficients of polynomials which are fit to the real and imaginary components respectively. The order of the polynomial is chosen for each z^2 separately to minimize the χ^2/d.o.f. As an example, the first and second moments calculated on the ensemble $a091m170$ are shown in Fig. 2. The z^2 dependence of the PDF moments resulting from this procedure can be used to check for the presence of significant higher twist effects, which do not seem to be present.

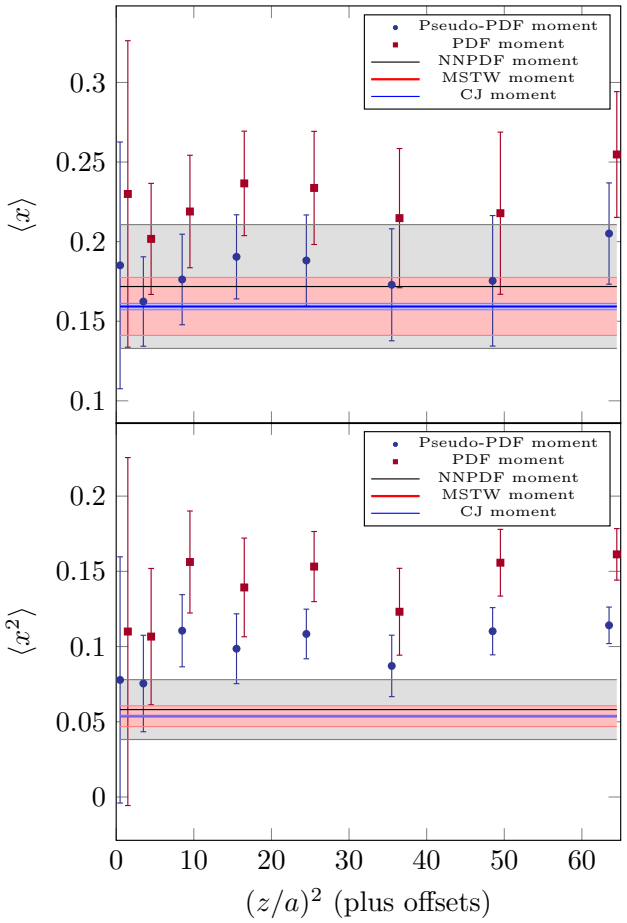

FIG. 2. The first two moments of the pseudo and the $\overline{\rm MS}$ lightcone PDF computed from the ensemble $a091m170$, compared to phenomenologically determined PDF moments from the NLO global fit CJ15nlo [55], the NNLO global fits MSTW2008nnlo68cl_nf4 [56] and NNPDF31_nnlo_pch_as_0118_mc_164 [57] all evolved to 2 GeV.

Extrapolation to the physical pion mass — In order to determine the valence PDF for physical pion mass, our

results must be extrapolated to 135 MeV. For each ensemble, a pseudo-dataset with 150 points is generated assuming a Gaussian distribution with the jackknife estimated mean and covariance. These data are fit, independently for each z, to a polynomial which is then used to extrapolate to 135 MeV. The functional form used is

$$\mathfrak{M}(\nu, z^2) = \left(1 + \sum_{n=1}^{N_C} c_n T_{2n}(\nu)\right)\left[1 + m\sum_{n=1}^{N_m} d_n \nu^{2n}\right] \quad (13)$$

where $T_i(x)$ are Chebyshev polynomials and m is the pion mass. The number of terms, N_C and N_m, is determined by minimizing the resulting χ^2/d.o.f. Several other functional forms have also been tried. These include forms with quadratic and logarithmic pion mass dependence. In addition, a mass-dependent finite volume correction term was added to Eq. (13). All of these forms gave results which are largely consistent with each other, except the functional form with the logarithm which consistently had a worse χ^2/d.o.f. Of all of those forms, the one in Eq. (13) consistently had the lowest χ^2/d.o.f. The reduced pseudo-ITD extrapolated to 135 MeV is shown in Fig. 3.

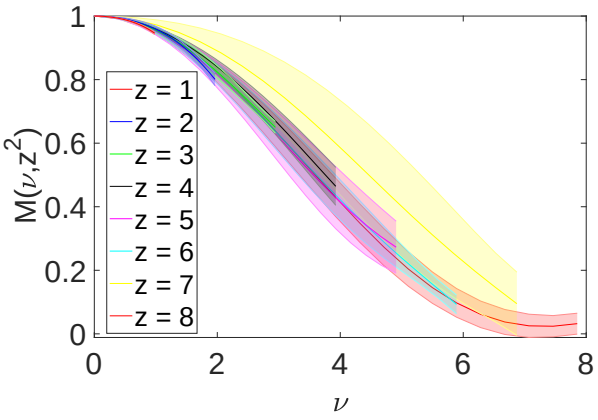

FIG. 3. The real component of the reduced pseudo-ITD data is fit to the functional form in Eq. (13) and extrapolated to 135 MeV, independently for each z. Due to the mild pion mass dependence, the resulting extrapolations differ only slightly from the original data.

Matching to $\overline{MS}$ — Similarly to what was done in Ref. [42] for the heavier pion masses, the matching of the reduced pseudo-ITD to the lightcone $\overline{\text{MS}}$ ITD at a given scale μ, is carried out via an inversion of Eq. (4) by exchanging $Q(\nu,\mu)$ and $\mathfrak{M}(\nu, z^2)$ and flipping the sign of α_s

$$Q(\nu,\mu) = \mathfrak{M}(\nu, z^2)\frac{\alpha_s C_F}{2\pi}\int_0^1 du\, \mathfrak{M}(u\nu, z^2) \times \left[\ln\left(z^2\mu^2\frac{e^{2\gamma_E+1}}{4}\right)B(u) + L(u)\right]. \quad (14)$$

By applying the matching, we obtain a set of z^2-independent curves for $Q(\nu,\mu)$ at $\mu = 2$ GeV, shown in Fig. 4a. The slight z^2-dependence of the lattice data (at small distances) has been entirely compensated by the $\ln z^2$ term, indicating that DGLAP evolution is present in our data [38, 45].

As seen in the moments, the matching procedure has a small effect on the distribution. The contributions from the convolution of B and L with the reduced pseudo-ITD appear with opposite signs. The convolution with L is slightly larger in magnitude, but by a factor which is approximately the same as the logarithmic coefficient of B. This feature may just be a coincidence at NLO, but it hints that higher order corrections may also be small. An NNLO or non-perturbative matching is required to check the effects of the perturbative truncation on the matching. These perturbative effects are of $\mathcal{O}(\alpha_s/\pi) \sim 0.1$, as expected.

Determination of the PDF — The inversion of the Fourier transform defining the ITD, given a finite amount of data, constitutes an ill-posed problem which can only be resolved by including additional information. As was shown in [41], the direct inverse Fourier transform can lead to numerical artifacts. Many techniques have been proposed of how to accurately calculate a PDF from lattice data [18, 24, 41, 58]. This issue also occurs in the determination of the PDF from experimental data.

The approach which is used here (and is common amongst phenomenological determinations) is to include information in the form of a model-dependent PDF parametrization. We have used two different functions of the form

$$f(x) = \frac{1}{N}x^a(1-x)^b(1+cx^n), \quad (15)$$

where $n = 0.5$ or 1 and N normalizes the PDF. Other functional forms were tried, but resulted in Ioffe time distributions with erroneous large ν behaviors. This functional form includes parameters a, b to capture the dominant small- and large-x behavior and also the parameter c to allow deviations in the intermediate x range. The average of the 3-parameter fits are shown in Fig. 4 and their difference is used to estimate the systematic error.

The PDF obtained from this fit, for $x \gtrsim 0.1$ is larger than the phenomenological fits. This feature is consistent with the larger value of the second moment 0.095(6) for this fit compared to the global fits in Fig. 2. Other remaining systematic errors could explain this discrepancy. This calculation was performed on ensembles with a fairly coarse lattice spacing and uses data with $ap \sim O(1)$. Discretization errors have been shown [42] to be potentially significant. Future calculations at smaller lattice spacings are required to control these effects. There also exist potentially notable finite volume corrections.

Conclusions. — We presented the first calculation of the nucleon PDF based on the method of Ioffe time pseudo-

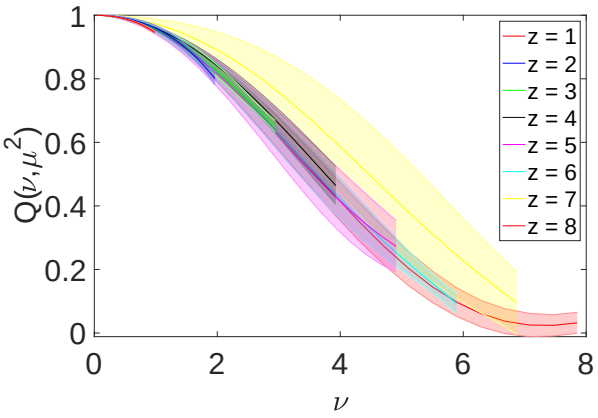

(a)

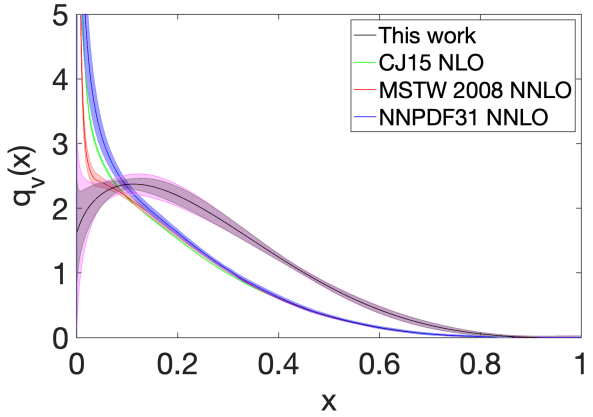

(b)

FIG. 4. (Upper) The $\overline{\text{MS}}$ ITD matched to 2 GeV from the reduced pseudo-ITD results extrapolated to the physical pion mass. (Lower) The nucleon valence distribution obtained from fitting the ITD to the form in Eq. (15). The gray band is just the statistical error and the magenta band includes additionally the systematic error originating from the choice of fitting function. The results are compared to phenomenological determinations from the NLO global fit CJ15nlo [55] (green), and the NNLO global fits MSTW2008nnlo68cl_nf4 [56] (red) and NNPDF31_nnlo_pch_as_0118_mc_164 [57] (blue) at a reference scale of 2 GeV.

distributions and performed at the physical pion mass. This was an important step that had to be taken in order to have a more meaningful comparison with the pertinent phenomenological results. Also, by studying three ensembles with different pion masses, we were able to investigate the dependence of the ITD on the pion mass. We saw that it is relatively mild compared to expectations stemming from the studies of $\langle x \rangle$ [59] and calculations of quasi-PDFs [14].

Compared to similar studies, our analysis capitalizes on three key factors. First, the ratio of matrix elements that yields a clean way to avoid all pitfalls and systematics of fixed gauge non-perturbative renormalization. Second, the short distance factorization, that allows for matching to $\overline{\text{MS}}$ without relying on large momentum data with their large statistical noise and potential discretization errors. Third, the summation method, that allows for a better control of the excited state contamination. Having studied finite volume effects and discretization errors in [42], in our upcoming work we plan to study in a systematic way the continuum extrapolation as well as effects stemming from excited state contaminations.

Acknowledgements.— JK thanks R. Sufian for helpful comments. This work is supported by Jefferson Science Associates, LLC under U.S. DOE Contract #DE-AC05-06OR23177. KO was supported in part by U.S. DOE grant #DE-FG02-04ER41302. AR was supported in part by U.S. DOE Grant #DE-FG02-97ER41028. J.K. was supported in part by the U.S. Department of Energy under contract DE-FG02-04ER41302, Department of Energy Office of Science Graduate Student Research fellowships, through the U.S. Department of Energy, Office of Science, Office of Workforce Development for Teachers and Scientists, Office of Science Graduate Student Research (SCGSR) program and is supported by U.S. Department of Energy grant DE-SC0011941. The authors gratefully acknowledge the computing time granted by the John von Neumann Institute for Computing (NIC) and provided on the supercomputer JURECA at Jülich Supercomputing Centre (JSC) [60]. This work was performed in part using computing facilities at the College of William and Mary which were provided by contributions from the National Science Foundation (MRI grant PHY-1626177), the Commonwealth of Virginia Equipment Trust Fund and the Office of Naval Research. The authors acknowledge William & Mary Research Computing for providing computational resources and/or technical support that have contributed to the results reported within this paper. In addition, this work used resources at NERSC, a DOE Office of Science User Facility supported by the Office of Science of the U.S. Department of Energy under Contract #DE-AC02-05CH11231, as well as resources of the Oak Ridge Leadership Computing Facility at the Oak Ridge National Laboratory, which is supported by the Office of Science of the U.S. Department of Energy under Contract No. #DE-AC05-00OR22725.

[1] J. Gao, L. Harland-Lang, and J. Rojo, Phys. Rept. **742**, 1 (2018), arXiv:1709.04922 [hep-ph].
[2] X. Ji, Phys. Rev. Lett. **110**, 262002 (2013).
[3] H.-W. Lin, J.-W. Chen, S. D. Cohen, and X. Ji, Phys. Rev. **D91**, 054510 (2015), arXiv:1402.1462 [hep-ph].
[4] J.-W. Chen, S. D. Cohen, X. Ji, H.-W. Lin, and J.-H. Zhang, Nucl. Phys. **B911**, 246 (2016), arXiv:1603.06664 [hep-ph].
[5] C. Alexandrou, K. Cichy, V. Drach, E. Garcia-Ramos, K. Hadjiyiannakou, K. Jansen, F. Stef-

fens, and C. Wiese, Phys. Rev. **D92**, 014502 (2015), arXiv:1504.07455 [hep-lat].
[6] C. Alexandrou, K. Cichy, M. Constantinou, K. Hadjiyiannakou, K. Jansen, F. Steffens, and C. Wiese, Phys. Rev. **D96**, 014513 (2017), arXiv:1610.03689 [hep-lat].
[7] C. Monahan and K. Orginos, JHEP **03**, 116 (2017), arXiv:1612.01584 [hep-lat].
[8] J.-H. Zhang, J.-W. Chen, X. Ji, L. Jin, and H.-W. Lin, Phys. Rev. **D95**, 094514 (2017), arXiv:1702.00008 [hep-lat].
[9] C. Alexandrou, K. Cichy, M. Constantinou, K. Hadjiyiannakou, K. Jansen, H. Panagopoulos, and F. Steffens, Nucl. Phys. **B923**, 394 (2017), arXiv:1706.00265 [hep-lat].
[10] J. Green, K. Jansen, and F. Steffens, Phys. Rev. Lett. **121**, 022004 (2018), arXiv:1707.07152 [hep-lat].
[11] I. W. Stewart and Y. Zhao, Phys. Rev. **D97**, 054512 (2018), arXiv:1709.04933 [hep-ph].
[12] C. Monahan, Phys. Rev. **D97**, 054507 (2018), arXiv:1710.04607 [hep-lat].
[13] W. Broniowski and E. Ruiz Arriola, Phys. Rev. **D97**, 034031 (2018), arXiv:1711.03377 [hep-ph].
[14] C. Alexandrou, K. Cichy, M. Constantinou, K. Jansen, A. Scapellato, and F. Steffens, Phys. Rev. Lett. **121**, 112001 (2018), arXiv:1803.02685 [hep-lat].
[15] J.-W. Chen, L. Jin, H.-W. Lin, Y.-S. Liu, Y.-B. Yang, J.-H. Zhang, and Y. Zhao, (2018), arXiv:1803.04393 [hep-lat].
[16] C. Alexandrou, K. Cichy, M. Constantinou, K. Jansen, A. Scapellato, and F. Steffens, Phys. Rev. **D98**, 091503 (2018), arXiv:1807.00232 [hep-lat].
[17] C. Alexandrou, K. Cichy, M. Constantinou, K. Hadjiyiannakou, K. Jansen, A. Scapellato, and F. Steffens, Phys. Rev. **D99**, 114504 (2019), arXiv:1902.00587 [hep-lat].
[18] T. Izubuchi, L. Jin, C. Kallidonis, N. Karthik, S. Mukherjee, P. Petreczky, C. Shugert, and S. Syritsyn, Phys. Rev. **D100**, 034516 (2019), arXiv:1905.06349 [hep-lat].
[19] J. R. Green, K. Jansen, and F. Steffens, (2020), arXiv:2002.09408 [hep-lat].
[20] Y. Chai *et al.*, (2020), arXiv:2002.12044 [hep-lat].
[21] W. Detmold and C. J. D. Lin, Phys. Rev. **D73**, 014501 (2006), arXiv:hep-lat/0507007 [hep-lat].
[22] V. Braun and D. Müller, Eur. Phys. J. **C55**, 349 (2008), arXiv:0709.1348 [hep-ph].
[23] A. J. Chambers, R. Horsley, Y. Nakamura, H. Perlt, P. E. L. Rakow, G. Schierholz, A. Schiller, K. Somfleth, R. D. Young, and J. M. Zanotti, Phys. Rev. Lett. **118**, 242001 (2017), arXiv:1703.01153 [hep-lat].
[24] J. Liang, T. Draper, K.-F. Liu, A. Rothkopf, and Y.-B. Yang, (2019), arXiv:1906.05312 [hep-ph].
[25] Y.-Q. Ma and J.-W. Qiu, Phys. Rev. Lett. **120**, 022003 (2018), arXiv:1709.03018 [hep-ph].
[26] G. S. Bali *et al.*, *Proceedings, 35th International Symposium on Lattice Field Theory (Lattice 2017): Granada, Spain, June 18-24, 2017*, Eur. Phys. J. **C78**, 217 (2018), arXiv:1709.04325 [hep-lat].
[27] G. S. Bali, V. M. Braun, B. Gläßle, M. Göckeler, M. Gruber, F. Hutzler, P. Korcyl, A. Schäfer, P. Wein, and J.-H. Zhang, Phys. Rev. **D98**, 094507 (2018), arXiv:1807.06671 [hep-lat].
[28] R. S. Sufian, J. Karpie, C. Egerer, K. Orginos, J.-W. Qiu, and D. G. Richards, Phys. Rev. **D99**, 074507 (2019), arXiv:1901.03921 [hep-lat].
[29] G. S. Bali *et al.* (RQCD), Eur. Phys. J. **A55**, 116 (2019), arXiv:1903.12590 [hep-lat].
[30] R. S. Sufian, C. Egerer, J. Karpie, R. G. Edwards, B. Joó, Y.-Q. Ma, K. Orginos, J.-W. Qiu, and D. G. Richards, (2020), arXiv:2001.04960 [hep-lat].
[31] H.-W. Lin *et al.*, Prog. Part. Nucl. Phys. **100**, 107 (2018), arXiv:1711.07916 [hep-ph].
[32] K. Cichy and M. Constantinou, Adv. High Energy Phys. **2019**, 3036904 (2019), arXiv:1811.07248 [hep-lat].
[33] C. Monahan, *36th International Symposium on Lattice Field Theory (Lattice 2018) East Lansing, MI, United States, July 22-28, 2018*, PoS **LATTICE2018**, 018 (2018), arXiv:1811.00678 [hep-lat].
[34] J.-W. Qiu, in *8th International Conference on Quarks and Nuclear Physics (QNP2018) Tsukuba, Japan, November 13-17, 2018* (2019) arXiv:1903.11902 [hep-ph].
[35] A. V. Radyushkin, Phys. Rev. **D96**, 034025 (2017), arXiv:1705.01488 [hep-ph].
[36] B. L. Ioffe, Phys. Lett. **30B**, 123 (1969).
[37] V. Braun, P. Gornicki, and L. Mankiewicz, Phys. Rev. **D51**, 6036 (1995), arXiv:hep-ph/9410318 [hep-ph].
[38] K. Orginos, A. Radyushkin, J. Karpie, and S. Zafeiropoulos, Phys. Rev. **D96**, 094503 (2017), arXiv:1706.05373 [hep-ph].
[39] J. Karpie, K. Orginos, A. Radyushkin, and S. Zafeiropoulos, *Proceedings, 35th International Symposium on Lattice Field Theory (Lattice 2017): Granada, Spain, June 18-24, 2017*, EPJ Web Conf. **175**, 06032 (2018), arXiv:1710.08288 [hep-lat].
[40] J. Karpie, K. Orginos, and S. Zafeiropoulos, JHEP **11**, 178 (2018), arXiv:1807.10933 [hep-lat].
[41] J. Karpie, K. Orginos, A. Rothkopf, and S. Zafeiropoulos, JHEP **04**, 057 (2019), arXiv:1901.05408 [hep-lat].
[42] B. Joó, J. Karpie, K. Orginos, A. Radyushkin, D. Richards, and S. Zafeiropoulos, JHEP **12**, 081 (2019), arXiv:1908.09771 [hep-lat].
[43] B. Joó, J. Karpie, K. Orginos, A. V. Radyushkin, D. G. Richards, R. S. Sufian, and S. Zafeiropoulos, Phys. Rev. **D100**, 114512 (2019), arXiv:1909.08517 [hep-lat].
[44] A. V. Radyushkin, (2019), arXiv:1912.04244 [hep-ph].
[45] A. Radyushkin, Phys. Rev. **D98**, 014019 (2018), arXiv:1801.02427 [hep-ph].
[46] J.-H. Zhang, J.-W. Chen, and C. Monahan, Phys. Rev. **D97**, 074508 (2018), arXiv:1801.03023 [hep-ph].
[47] T. Izubuchi, X. Ji, L. Jin, I. W. Stewart, and Y. Zhao, Phys. Rev. **D98**, 056004 (2018), arXiv:1801.03917 [hep-ph].
[48] G. Altarelli and G. Parisi, Nucl. Phys. **B126**, 298 (1977).
[49] R. Edwards, B. Joó, K. Orginos, D. Richards, and F. Winter, U.S. 2+1 flavor clover lattice generation program (2016), unpublished.
[50] B. Yoon *et al.*, Phys. Rev. **D95**, 074508 (2017), arXiv:1611.07452 [hep-lat].
[51] C. R. Allton *et al.* (UKQCD), Phys. Rev. **D47**, 5128 (1993), arXiv:hep-lat/9303009 [hep-lat].
[52] G. S. Bali, B. Lang, B. U. Musch, and A. Schäfer, Phys. Rev. **D93**, 094515 (2016), arXiv:1602.05525 [hep-lat].
[53] C. Bouchard, C. C. Chang, T. Kurth, K. Orginos, and A. Walker-Loud, Phys. Rev. **D96**, 014504 (2017), arXiv:1612.06963 [hep-lat].
[54] Z.-Y. Fan, Y.-B. Yang, A. Anthony, H.-W. Lin, and K.-F. Liu, Phys. Rev. Lett. **121**, 242001 (2018), arXiv:1808.02077 [hep-lat].
[55] A. Accardi, L. T. Brady, W. Melnitchouk, J. F.

Owens, and N. Sato, Phys. Rev. **D93**, 114017 (2016), arXiv:1602.03154 [hep-ph].
[56] A. D. Martin, W. J. Stirling, R. S. Thorne, and G. Watt, Eur. Phys. J. **C63**, 189 (2009), arXiv:0901.0002 [hep-ph].
[57] R. D. Ball *et al.* (NNPDF), Eur. Phys. J. **C77**, 663 (2017), arXiv:1706.00428 [hep-ph].
[58] K. Cichy, L. Del Debbio, and T. Giani, JHEP **10**, 137 (2019), arXiv:1907.06037 [hep-ph].
[59] M. Constantinou, *Proceedings, 32nd International Symposium on Lattice Field Theory (Lattice 2014): Brookhaven, NY, USA, June 23-28, 2014*, PoS **LATTICE2014**, 001 (2015), arXiv:1411.0078 [hep-lat].
[60] Jülich Supercomputing Centre, Journal of large-scale research facilities **4** (2018), 10.17815/jlsrf-4-121-1.